Birch-Type Reduction of Arenes in 2-Propanol Catalyzed by Zero-Valent Iron and Platinum on Carbon

Yoshinari Sawama,[a]* Kazuho Ban,[a] Kazuhiro Akutsu-Suyama,[b] Hiroki Nakata,[a] Misato Mori,[a] Tsuyoshi Yamada,[a] Takahiro Kawajiri,[a] Naoki Yasukawa,[a] Kwihwan Park,[a] Yasunari Monguchi,[a] Yukio Takagi,[c] Masatoshi Yoshimura,[c] and Hironao Sajiki[a]*

[a] Laboratory of Organic Chemistry, Gifu Pharmaceutical University, 1-25-4, Daigaku-nishi, Gifu, 501-1196, Japan

[b] Neutron Science and Technology Center, Comprehensive Research Organization for Science and Society (CROSS), 162-1 Shirakata, Tokai-Mura, Naka-gun, Ibaraki 319-1106, Japan

[c] Catalyst Development Center, N. E. Chemcat Corporation, 678 Ipponmatsu, Numazu, Shizuoka 410-0314, Japan

E-mail: sawama@gifu-pu.ac.jp; sajiki@gifu-pu.ac.jp

Contents

1. XANES, EXAFS, and PNR analysis.

2. XPS of fresh 10% Pt/C.

3. Effect of usage of 2-PrOH

4. Mechanism study using cyclohexadiene derivative (9) as a substrate.

5. References.

6. ^{1}H NMR spectra of products.

1. XANES, EXAFS, and PNR analysis.

The local structure of Fe atom and the oxidation state of Fe and Pt were studied by the extended X-ray absorption fine structure (EXAFS), X-ray absorption near edge spectroscopy (XANES) and polarized neutron reflectivity (PNR) analyses.[1] Because PNR analysis has been developed as one of the most important experimental methods for the analysis of magnetic structures, we can use it to elucidate whether the sample contains the bulk composition of Fe species after the arene reduction as the value of magnetic moment of Fe.

X-ray absorption fins structure (XAFS) measurements were performed using the fluorescence mode at the BL5S1 Hard X-ray EXAFS beamline station in Aichi Synchrotron Radiation Center (Aichi SR), Aichi Science & Technology Foundation, Aichi, Japan.[2] The synchrotron radiation was monochromatized by a Si(111) double-crystal monochromator. The incident X-rays were monitored by an ionization chamber (14 cm in length) filled with N_2 gas. The fluorescence X-rays were detected by a multi-element solid-state detector (19 elements), which was placed close to the sample surface. The Fe K-edge and Pt L_{III}-edge XAFS spectra were recorded within 6.81–8.21 keV (for Fe) and 11.25–12.65 keV (for Pt), respectively. Iron powder, 10 mM $FeCl_3$ aqueous solution, Pt foil, and 1mM $PtCl_4$ aqueous solution were used as the standard sample of XAFS analyses. Each sample was measured for 50 min. The XAFS spectra were analyzed using the WinXAS 3.1 program[3] according to a standard method.[4] Intensities of the XANES spectra were normalized using the post-edge higher energy region. Theoretical phase shifts and backscattering amplitude functions were generated using the FEFF8.00 code[5] from the crystallographic and EXAFS data for Fe-O and Fe-Fe bonds of Fe species.[6,7] All possible single scattering paths were taken into account in the curve fittings. The amplitude of the reduction factor, S_0^2, was fixed at 0.9.

The PNR measurements were performed on a BL17 SHARAKU reflectometer installed at the Materials and Life Science Experimental Facility (MLF) in J-PARC.[1,8] The incident beam power of the proton accelerator was 500 kW for all the measurements. Pulsed neutron beams were generated using a mercury target at 25 Hz, and the NR data were measured using the time-of-flight (TOF) technique. The neutron-source to sample distance was 15.5 m, and the sample to 3He gas point detector distance was 2.5 m. The wavelength (λ) range of the incident polarized neutron beam was tuned to be approximately $\lambda = 2.4 – 8.8$ Å using disk choppers. The incident angle was 0.3° and 0.8°, and the total exposure times for the measurements was 3 h. The covered Q_z range was $Q_z = 0.008 – 0.08$ Å^{-1}, where $Q_z = (4\pi/\lambda)\sin\theta$ (here, θ represents the incident angle). The samples were placed in a sample holder on the 1 tesla-magnet stage, which was installed at the center position of the sample rotation. A 25 mm beam footprint was maintained on the sample surface by using six kinds of incident slits. All the measurements were performed at room temperature with a uniform 1.0 Tesla magnetic field strength. The data reduction, normalization, and subtraction were performed using a program installed in BL17 SHARAKU that was developed for the TOF data. The sample solution was dropped onto a Si wafer

and the solution was evaporated in a desiccator. After the dry process, an another Si wafer was put on the sample coated Si wafer. Samples sandwiched between two Si wafers were used for the PNR measurements.

Figure S1(same as Figure 3(a) and (b) in the main text). (a) shows the Fe K-edge XANES spectra of samples. Figure S1(b) shows the plot of Fe K-edge absorption edge energy shift (eV) vs the valence (oxidation state) of Fe of samples. It is clear that the XANES spectra of aliovalent Fe with known structure and chemical formula are fit to linear combinations of pure Fe species.[9,10] Therefore, we can obtain the relative shift of the Fe K-edge absorption edge position corresponding to the change of Fe oxidation state, fitting the XANES spectra with the simple step function. According to the Fe K-edge XANES analysis, the mean Fe valence could be estimated to be 1.57 and 1.5 for samples Ⓐ and Ⓑ, respectively.
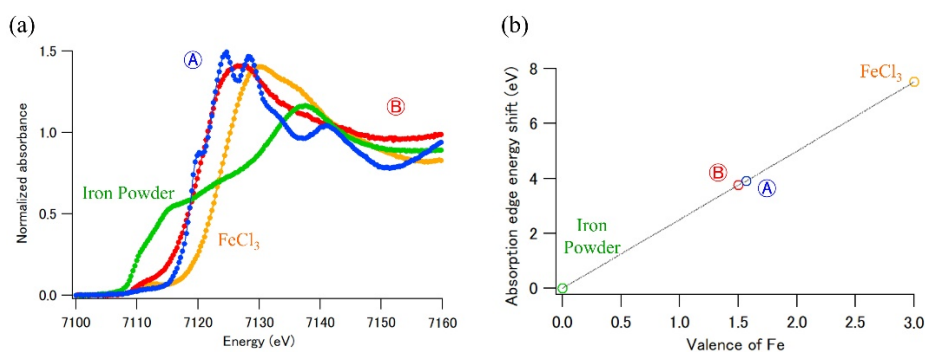
Figure S1. (a) Fe K-edge XANES spectra for various kinds of Fe samples (sample conditions are described in the main text). (b) The plot of Fe K-edge absorption edge energy shift (eV) vs the valence of Fe of the samples.

Figure S2 (same as Figure 4(a) and (b) in the main text). (a) shows the Pt L_{III}-edge XANES spectra of samples. Figure S2(b) shows the plot of Pt L_{III}-edge absorption edge energy shift (eV) vs the valence (oxidation state) of Pt of samples. The intensities of the white lines for samples Ⓐ and Ⓑ are higher than that for Pt foil. It indicated that the samples were oxidized during the reaction.[11] In addition, since it was reported that the XANES spectra of aliovalent Pt with known structure and chemical formula are fit to linear combinations of pure Pt species,[12] we estimated the mean Pt valence by analyzing the XANES data. In the Pt L_{III}-edge XANES analysis, we could obtain the relative shift of the Pt L_{III}-edge absorption peak position for the Pt samples. According to the Pt L_{III}-edge XANES analysis, the mean Pt valence could be estimated to be 1.51 and 1.32 for samples Ⓐ and Ⓑ, respectively.
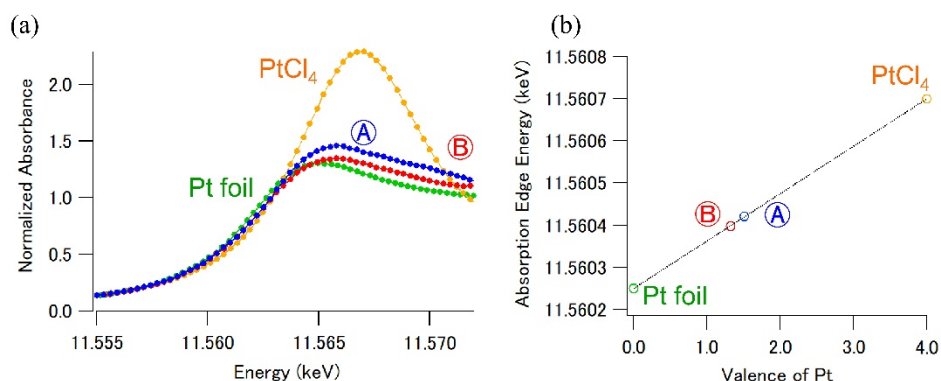
Figure S2. (a) Pt L_{III}-edge XANES spectra for various kinds of Pt samples (sample conditions are described in the main text). (b) The plot of Pt L_{III}-edge absorption edge energy shift (eV) vs the valence of Pt of the samples.

EXAFS analyses were performed to determine the valence state and the average local structure of Fe in the reaction mixture.

Table S1. EXAFS structural parameters for various kinds of Fe samples obtained by curve fitting.

Sample	Model	N	R (Å)	σ^2 (Å^2)	ΔE_0	Residual (%)
Fe Powder	Fe-O	2.08	1.88	0.002	6.0	7.1
	Fe-Fe	4.67	2.21	0.015	10	
	Fe-Fe	0.44	2.57	0.003	-10	
FeCl$_3$	Fe-O	2.21	1.84	0.009	-0.1	2.1
	Fe-O	4.23	1.99	0.002	-8.5	
Sample Ⓐ	Fe-O	5.29	2.05	0.004	-5.0	12.0
	Fe-Fe	1.97	3.06	0.015	10	
Sample Ⓑ	Fe-O	1.51	1.97	0.003	2.8	4.6
	Fe-O	1.92	2.15	0.003	-4.4	
	Fe-Fe	0.79	2.48	0.004	-9.4	
	Fe-Fe	0.37	2.88	0.006	1.2	
	Fe-Fe (or Fe-O-Fe)	1.60	3.10	0.008	10	

N: coordination number, R(Å): bond distance, σ^2(Å^2): Debye-Waller factor squared, ΔE_0 (eV): energy shift parameter, residual: $\{\sum |y_{exp(i)} - y_{theo(i)}| / \sum |y_{exp(i)}|\} \times 100$ (%) (y denotes experimental and theoretical data points).
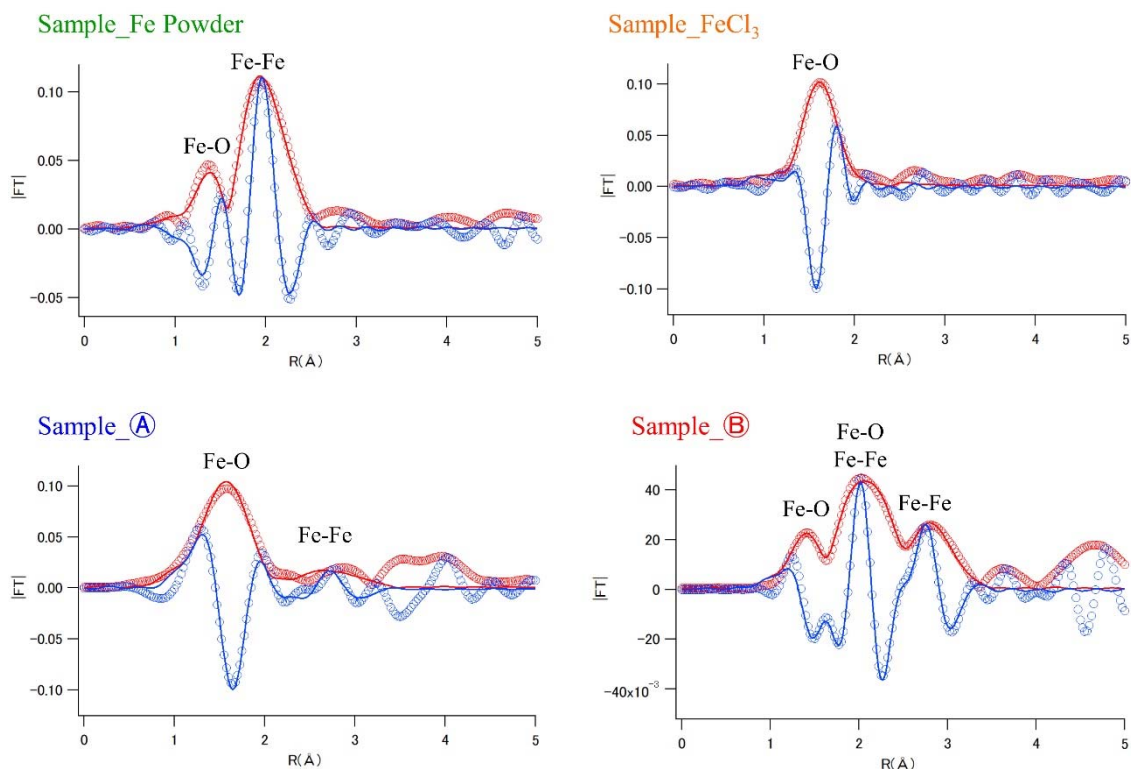
Figure S3. The corresponding magnitude (red) and imaginary part (blue) of the Fourier-transformed (FT) Fe *K*-edge EXAFS for various kinds of Fe samples. Solid lines and circles indicate the experimental data and theoretical fit, respectively. The phase shift in the FT data was not corrected.

Figure S3 shows the corresponding magnitude and imaginary part of the Fourier-transformed (FT) Fe *K*-edge EXAFS for various kinds of Fe samples. Because oxygen and Fe species can interact with another Fe species in these samples, both Fe-O and Fe-Fe models were used to fit the EXAFS data. Note that because the concentration of FeCl$_3$ is very low in the solution, it is obvious that there is no distinguishable Fe-Cl interaction in the sample.[13,14] The FT spectra exhibited three peaks at 1.5, 2.0, and 2.7 Å. The first peak at 1.5 Å can be clearly assigned to a Fe-O interaction and the other peaks at 2.0 and 2.6 Å can also be clearly assigned to Fe-Fe interactions.[7,15] Table 1 shows the EXAFS structural parameters obtained from the analysis. The fitting results showed that the first interaction shell of Fe consisted of oxygen atoms with a Fe–O distance of 1.84–2.15 Å in all samples. This result indicates that oxidized iron species such as iron oxide or iron hydroxide were generated after the reaction. In addition, the second interaction shell of Fe consisted of Fe atoms with a Fe–Fe distance of 2.21–3.10 Å in sample Ⓐ, Ⓑ, and Fe powder. Considering the small interaction number of Fe-Fe in sample Ⓐ, dominant Fe species would be Fe^{2+}. However, since the interaction number of Fe-Fe in sample Ⓑ is comparatively large, it is not appropriate to make certain the mean valence of Fe by the

EXAFS results. Therefore, the EXAFS data suggested that Fe^0 was oxidized after the reaction process, and Fe^{2+} species was mainly generated in sample Ⓐ.

PNR analyses was performed to determine the change of the magnetic structure of Fe powder of the reaction mixture. Figure S4. The PNR profiles of samples before and after the arene reduction. A small difference between R^{++} and R^{--} was observed only in the fresh sample (before arene reduction). It indicated that the fresh sample contains Fe as a bulk configuration, and it was decomposed after the reaction process. It would be better to say that the decreasing of the magnetic structure could be due to the oxidation of Fe as a bulk configuration.
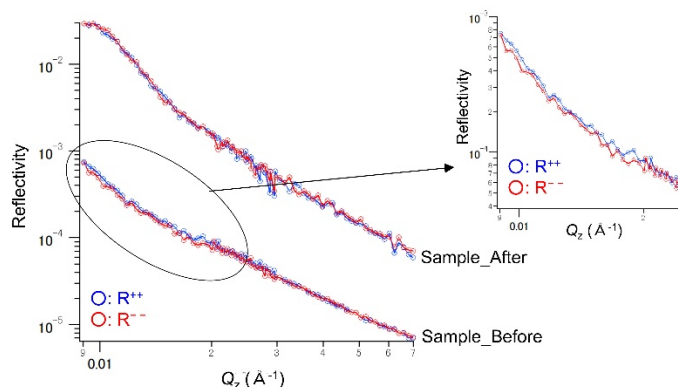
Figure S4. The PNR profiles of before and after the arene reduction samples. The circles represent the experimental data, and the PNR profiles of before the arene reduction sample are vertically shifted to avoid overlap.

In summary, XANES, EXAFS, and PNR analyses suggested that although the mean Fe valence could be estimated to be 1.57 for Ⓐ and 1.5 Ⓑ sample, it is reasonable to suppose that the dominant initial species of iron, Fe^0, was partially oxidized via the redox reaction process and the oxidized Fe^{2+} species would mainly be generated after the reaction.

2. XPS of fresh 10% Pt/C.
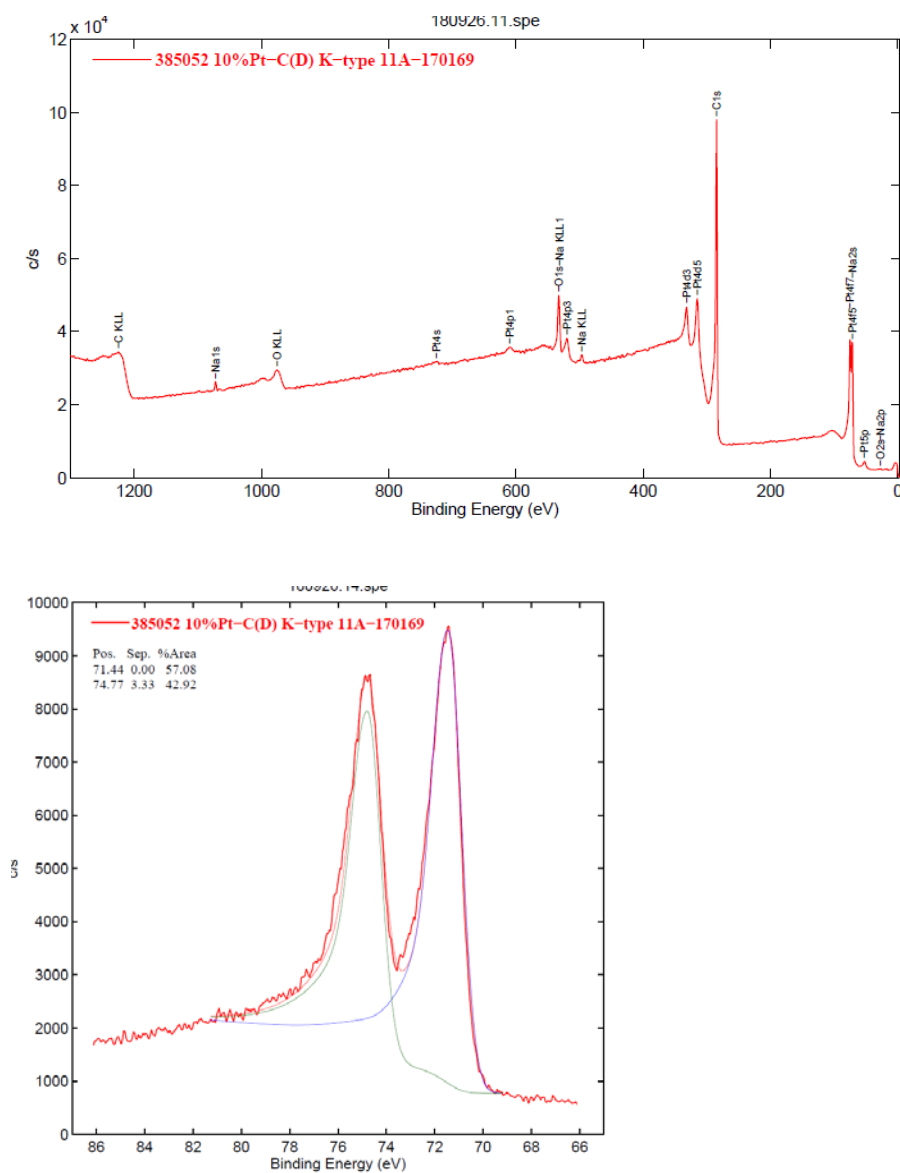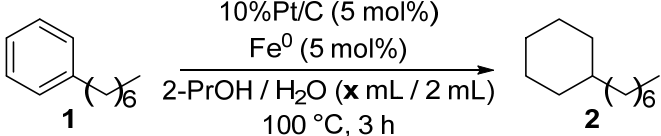

The zero valent of platinum is supported on carbon.

Reference

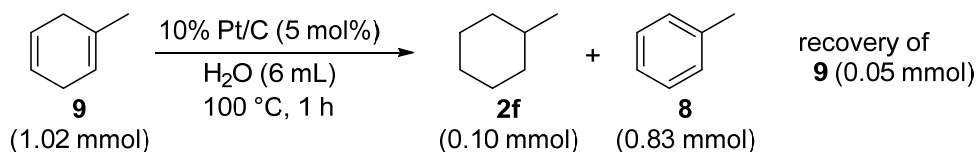|	Pt4f7/2
Pt	*71.1
PtO	73.8-74.2
PtO$_2$	*75.1

Figure S5. XPS spectra of fresh 10% Pd/C.

3. Effect of usage of 2-PrOH

Table S2. Effect of usage of 2-PrOH and the amount of H_2 generated in the sealed glass tube.

$$\text{1} \xrightarrow[\substack{\text{2-PrOH / H}_2\text{O (}x\text{ mL / 2 mL)}\\ 100\,°\text{C, 3 h}}]{\substack{10\%\text{Pt/C (5 mol\%)}\\ \text{Fe}^0\text{ (5 mol\%)}}} \text{2}$$

2-PrOH (x mL)	ratio (mol/mol)		internal H_2 (mmol)
	1	2	
4	0	100	0.33[a]
3	0	100	0.073
2	15	85	0.028

[a]For 6 h.

4. Reaction study of cyclohexadiene derivative (9).

$$\text{9} \xrightarrow[\substack{\text{H}_2\text{O (6 mL)}\\ 100\,°\text{C, 1 h}}]{10\%\text{ Pt/C (5 mol\%)}} \text{2f} + \text{8} \quad \text{recovery of 9 (0.05 mmol)}$$

9 (1.02 mmol) → 2f (0.10 mmol) + 8 (0.83 mmol)

A 30 mL co-plug test tube was sequentially charged with 1-methyl-1,4-cyclohexadiene (**9**; 96.2 mg, 1.02 mmol), 10 % Pt/C (97.6 mg, 0.050 mmol) and H_2O (6 mL), and the suspension was stirred at 100 °C. After stirring for 1 h, the mixture was cooled to room temperature and added anisole (100 µL) as an internal standard. The mixture was filtered through a membrane filter (Millipore, Millex®-LH, 0.2 µm) to remove catalysts. The filtrate was transferred to a 100 mL volumetric flask with Et_2O. 20 µL of sample was dissolve in 1.5 mL Et_2O. **2f**, **8** and **9** were detected by GC/MS and given in 0.10, 0.83 and 0.05 mmol, respectively.

Helium was employed as a carrier gas at the flow rate of 1.3 mL/min. The injector and detector temperatures were 220 °C. The column temperature was programmed to ramp from 40 °C (1 min hold) to 110 °C (2 min hold) at the rate of 5 °C/min. 1 µL of sample solution was injected (split; 1 : 10). The products were identified by their GC/MS retention times in comparison to those of authentic commercial samples. Retention time (min); 3.32 (methylcyclohexane), 4.16 (toluene), 4.21 (1-methyl-1,4-cyclohexadiene), 7.18 (internal standard (Anisole)).

5. References

1) Ukleev, V.; Suturin, S.; Nakajima, T.; Arima, T.; Saerbeck, T.; Hanashima, T.; Sitnikova, A.; Kirilenko, D.; Yakovlev, N.; Sokolov, N. Unveiling structural, chemical and magnetic interfacial peculiarities in ε-Fe_2O_3/GaN (0001) epitaxial films. *Sci. Rep.* **2018**, *8*, 8741.

2) Tabuchi, M.; Asakura, H.; Morimoto, H.; Watanabe, N.; Takeda, Y. Hard X-ray XAFS beamline, BL5S1, at AichiSR. *Journal of Physics: Conference Series* **2016**, *712*, 012027.

3) Ressler, T. WinXAS: a Program for X-ray absorption spectroscopy data analysis under MS-Windows. *J. Synchrotron Radiat.* **1998**, *5*, 118−122.

4) Jones, G. R.; George, J. M. The experience and evolution of trust: implications for cooperation and teamwork. *Endeavour* **1988**.

5) Ankudinov, A. L.; Rehr, J. J.; Conradson, S. D. Real-space multiple-scattering calculation and interpretation of X-ray-absorption near-edge structure. *Physical Review B*. **1998**, 7565−7576.

6) Waldmann, O.; Koch, R.; Schromm, S.; Schülein, J.; Müller, P.; Bernt, I.; Saalfrank, R. W.; Hampel, F.; Balthes, E. Magnetic anisotropy of a cyclic octanuclear Fe(III) cluster and magneto-structural correlations in molecular ferric wheels. *Inorg. Chem.* **2001**, *40*, 2986−2995.

7) Signorini, L.; Pasquini, L.; Savini, L.; Carboni, R.; Boscherini, F.; Bonetti, E.; Giglia, A.; Pedio, M.; Mahne, N.; Nannarone, S. Size-dependent oxidation in iron/iron oxide core-shell nanoparticles. *Phys. Rev. B* **2003**, *68*, 194523.

8) Akutsu, K.; Niizeki, T.; Nagayama, S.; Miyata, N.; Sahara, M.; Shimomura, A.; Yoshii, M.; Hasegawa, Y. Investigation of structure of a thin SiO_2 layer as an antifouling and corrosion-resistant coating. *J. Ceram. Soc. Japan* **2016**, *124*, 172−176.

9) Choi, S. H.; Wood, B. R.; Bell, A. T.; Janicke, M. T.; Ott, K. C. X-ray absorption fine structure analysis of the local environment of Fe in Fe/Al-MFI. *J. Phys. Chem. B* **2004**, 8970−8975.

10) Arčon, L.; Kolar, J.; Kodre, A.; Hanžel, D.; Strlič, M. XANES analysis of Fe valence in iron gall inks. *X-Ray Spectrom.* **2007**, 199-205.

11) Shishido, T.; Tanaka, T.; Hattori, H. State of platinum in zirconium oxide promoted by platinum and sulfate ions. *J. Catal.* **1997**, *172*, 24−33.

12) Tomita, A.: Shimizu, K.; Kato, K.; Akita, T.; Tai, Y. Mechanism of low-temperature CO oxidation on Pt/Fe-containing alumina catalysts pretreated with water. *J. Phys. Chem. C* **2013**, *117*, 1268−1277.

13) Zhu, M.; Puls, B. W.; Frandsen, C.; Kubicki, J. D.; Zhang, H.; Waychunas, G. A. In situ structural characterization of ferric iron dimers in aqueous solutions: identification of μ-oxo species. *Inrog. Chem.* **2013**, *52*, 6788−6797.

14) Asakura, K.; Nomura, M.; Kuroda, H. Fe *K*-Edge XANES and EXAFS of the X-Ray absorption spectra of $FeCl_3$ aqueous solutions. A structural study of the solute, iron(III) chloro complexes. *Bull.*

Chem. Soc. Jpn. **1985**, *58*, 1543−1550.

15) Shuvayev, A. T.; Helmer, B. Y.; Lyubeznova, T.; Kraizman, V. L.; Mirmilstein, A. S.; Kvacheva, L. D.; Novikov, Y. N.; Volpin, M. E. EXAFS study of graphite intercalation compounds with transition metals (Fe, Ni). *J. Phys. France* **1989**, *50*, 1145−1151.
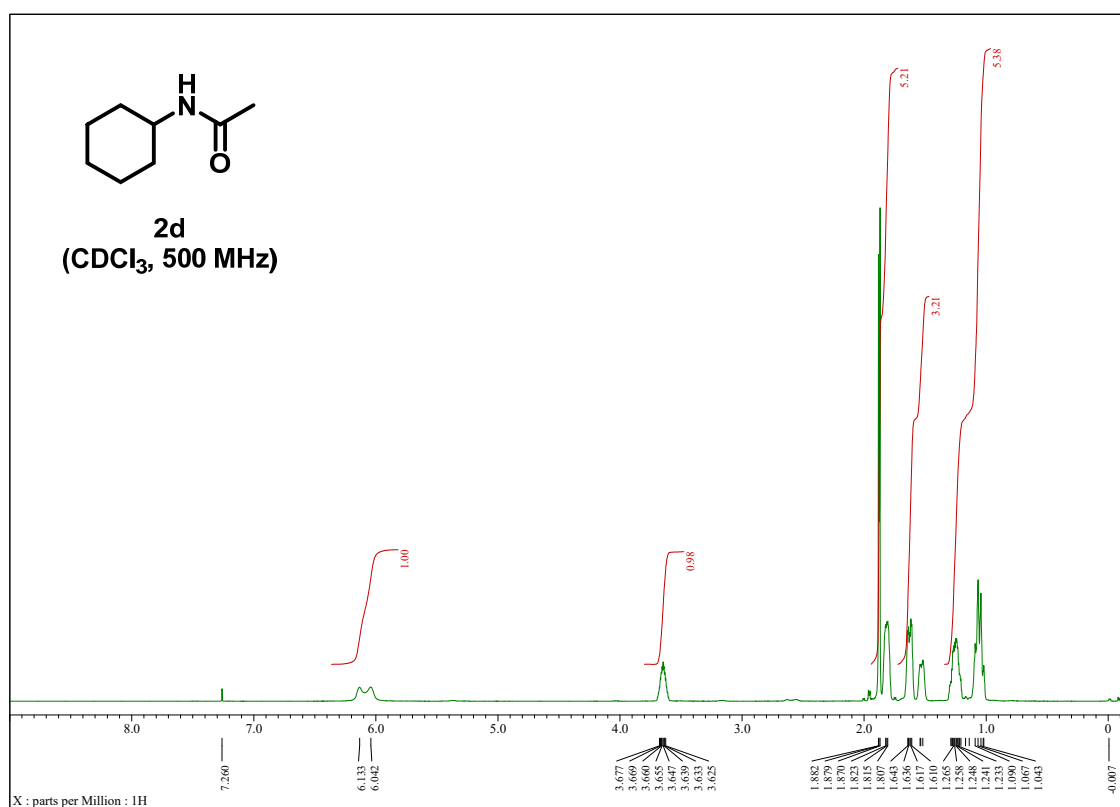
6. ¹H NMR spectra of products.

Figure S6. ¹H NMR of heptylcyclohexane (**2a**)

Figure S7. ¹H NMR of bicyclohexyl (**2b**)
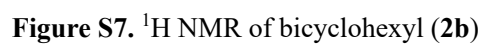
Figure S8. ^{1}H NMR of *tert*-butylcyclohexane (**2c**)

2c
(CDCl$_3$, 500 MHz)
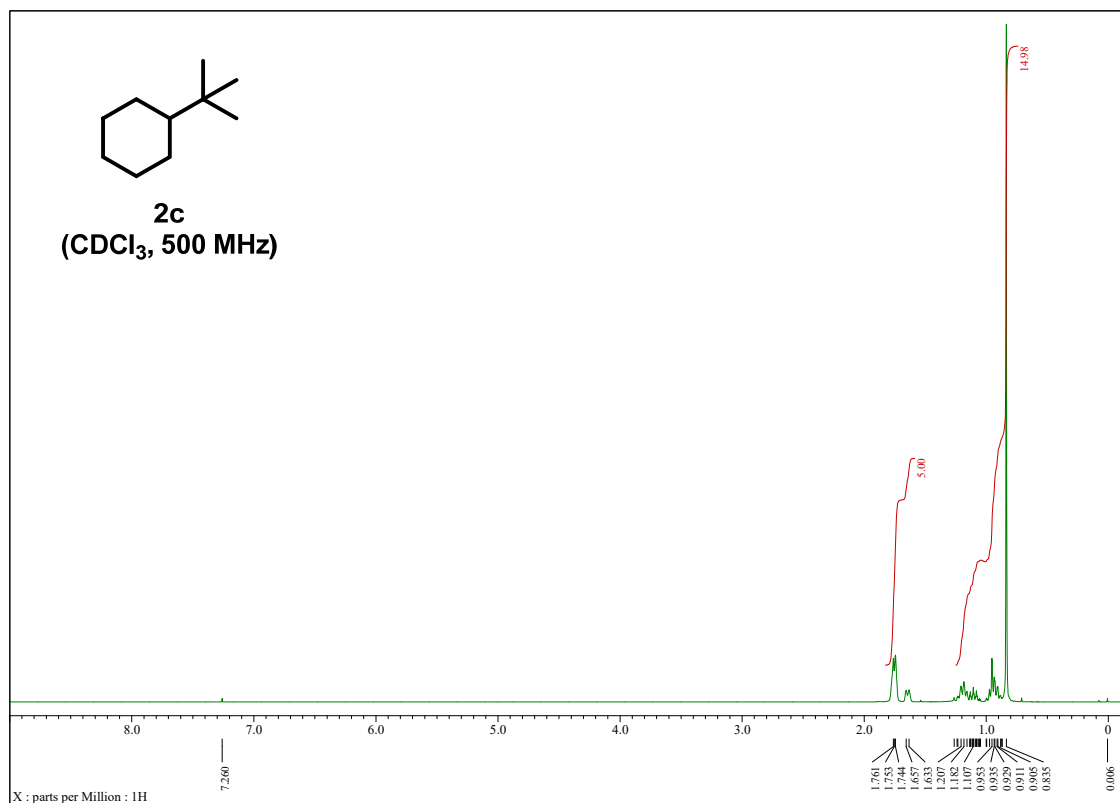
Figure S9. ^{1}H NMR of *N*-cyclohexylacetamide (**2d**)

2d
(CDCl$_3$, 500 MHz)

Figure S10. ^{1}H NMR of 1,2,3,4,5,6,7,8-octahydroanthracene (**2e**)

2e
(CDCl$_3$, 500 MHz)

X : parts per Million : 1H
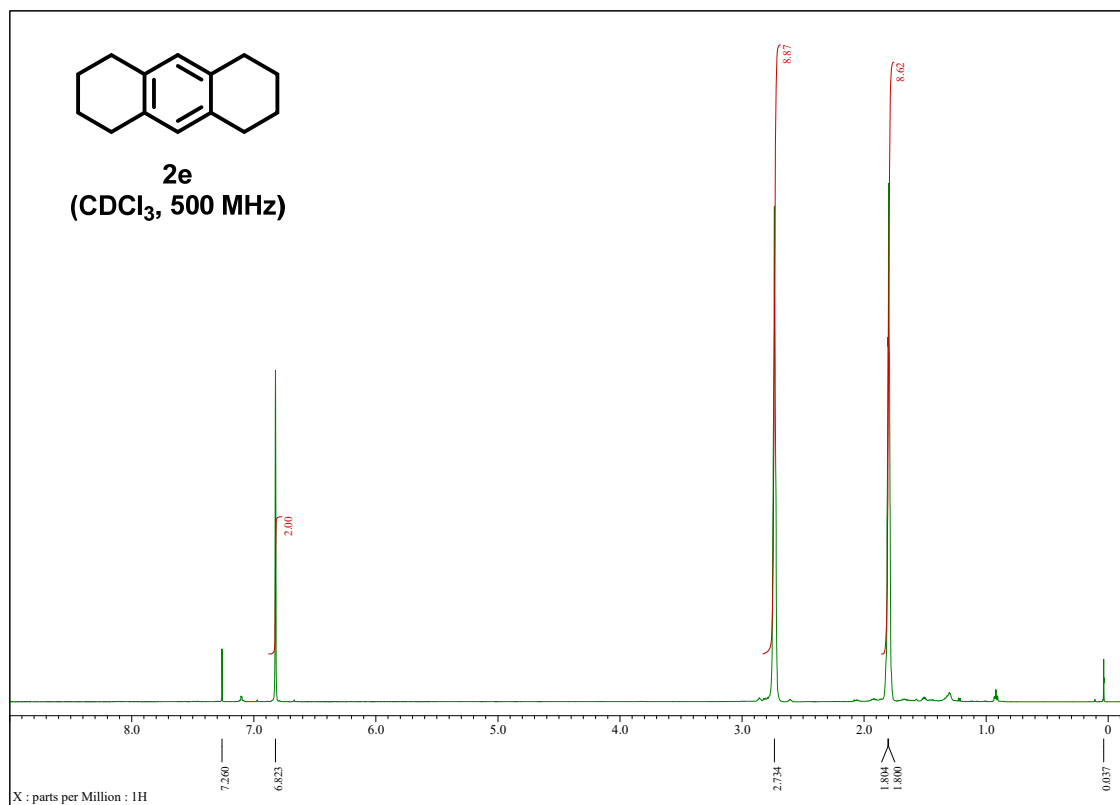
Figure S11. ^{1}H NMR of dibenzyl (**4**)

4
(CDCl$_3$, 400 MHz)

X : parts per Million : Proton
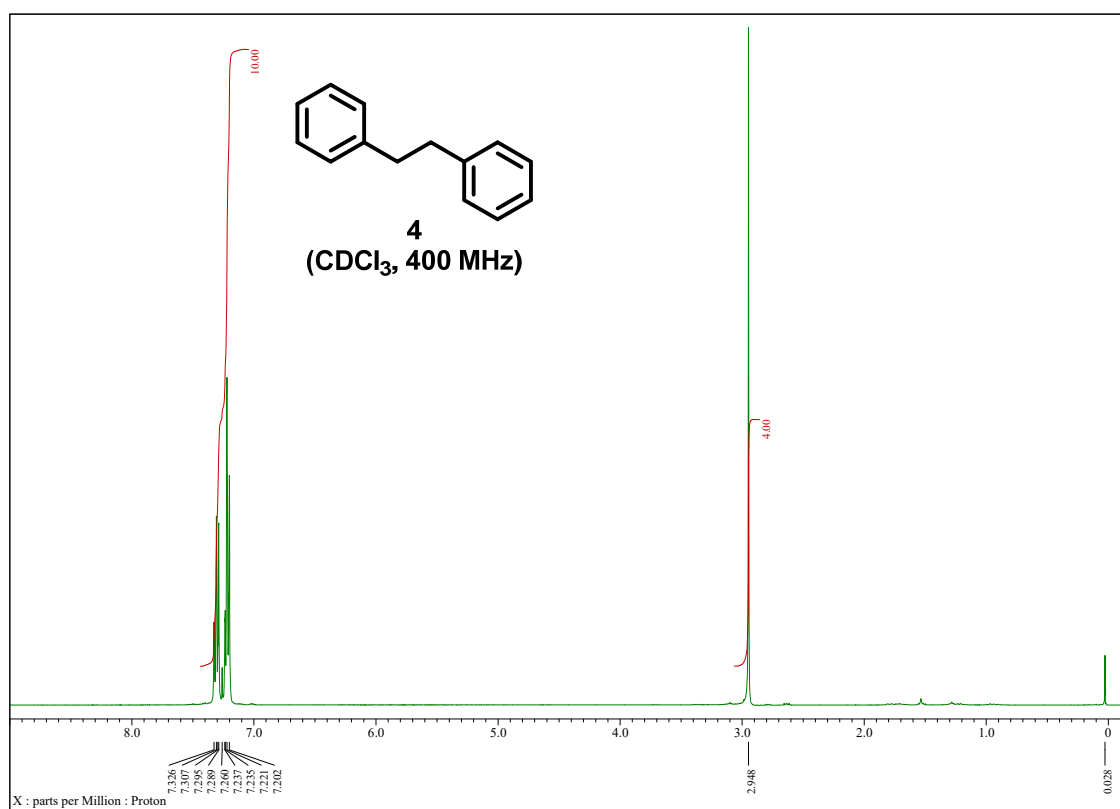
Figure S12. ^{1}H NMR of 1,2-dicyclohexylethane (**5**)

5
(CDCl$_3$, 400 MHz)

12.28
10.14
4.00

8.0 7.0 6.0 5.0 4.0 3.0 2.0 1.0 0

7.260

1.702
1.694
1.677
1.621
1.256
1.224
1.200
1.193
1.156
1.115
0.890
0.861
0.835

0.004

X : parts per Million : Proton
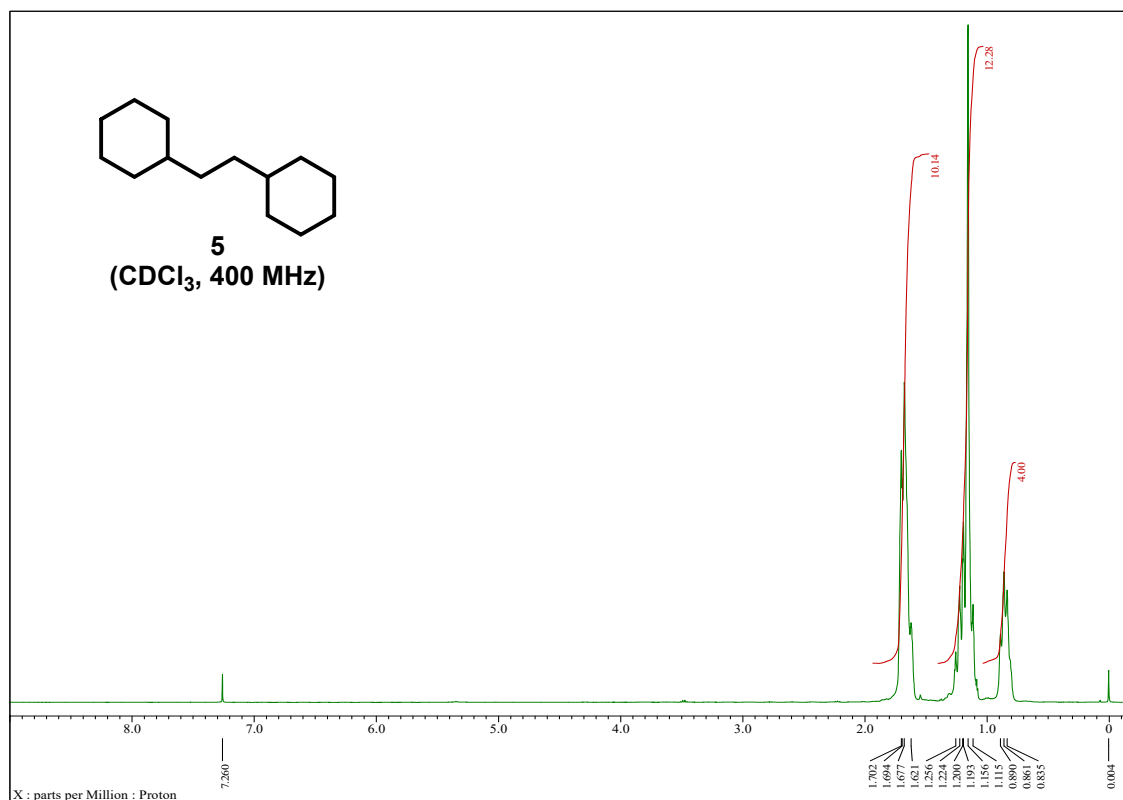
Figure S13. ^{1}H NMR of tetradecane (**7**)

Me⟍⟋Me
12
7
(CDCl$_3$, 400 MHz)

24.32

6.00

8.0 7.0 6.0 5.0 4.0 3.0 2.0 1.0 0

7.260

1.320
1.303
1.260
0.899
0.883
0.864

0.002

X : parts per Million : Proton